



# Seasonal effect on vertical positional by satellite laser ranging and Global Positioning System and on absolute gravity at the OCA geodetic station, Grasse, France

Jean-Marie Nicolas, J.-M. Nocquet, Camp Van, M. Van, T. Dam, J.-P. Boy, J. Hinderer, P. Gegout, E. Calais, M. Amalvict

## ► To cite this version:

Jean-Marie Nicolas, J.-M. Nocquet, Camp Van, M. Van, T. Dam, et al.. Seasonal effect on vertical positional by satellite laser ranging and Global Positioning System and on absolute gravity at the OCA geodetic station, Grasse, France. *Geophysical Journal International*, 2006, 167 (3), pp.1127-1137. 10.1111/j.1365-246X.2006.03205.x . hal-00407615

**HAL Id: hal-00407615**

**<https://hal.science/hal-00407615>**

Submitted on 19 Oct 2021

**HAL** is a multi-disciplinary open access archive for the deposit and dissemination of scientific research documents, whether they are published or not. The documents may come from teaching and research institutions in France or abroad, or from public or private research centers.

L'archive ouverte pluridisciplinaire **HAL**, est destinée au dépôt et à la diffusion de documents scientifiques de niveau recherche, publiés ou non, émanant des établissements d'enseignement et de recherche français ou étrangers, des laboratoires publics ou privés.



Distributed under a Creative Commons Attribution 4.0 International License

# Seasonal effect on vertical positioning by Satellite Laser Ranging and Global Positioning System and on absolute gravity at the OCA geodetic station, Grasse, France

J. Nicolas,<sup>1</sup> J.-M. Nocquet,<sup>2</sup> M. Van Camp,<sup>3</sup> T. van Dam,<sup>4</sup> J.-P. Boy,<sup>5</sup> J. Hinderer,<sup>5</sup> P. Gegout,<sup>5</sup> E. Calais<sup>6</sup> and M. Amalvict<sup>5</sup>

<sup>1</sup>Laboratoire de Géodésie et Géomatique (L2G), ESGT/CNAM, 1 Bd Pythagore, F-72000 Le Mans, France. E-mail: joelle.nicolas@esgt.cnam.fr

<sup>2</sup>CNRS – Géosciences Azur, Bât. 4, 250 Rue Albert Einstein, Les Lucioles 1, Sophia Antipolis, F-06560 Valbonne, France

<sup>3</sup>Royal Observatory of Belgium (ROB), Avenue Circulaire 3, B-1180 Brussels, Belgium

<sup>4</sup>Faculté des Sciences, de la Technologie et de la Communication, University of Luxembourg, 162a, avenue de la Faiënerie, L-1511 Luxembourg

<sup>5</sup>EOST/IPGS (UMR 7516 CNRS/ULP), 5 rue René Descartes, F-67084 Strasbourg Cedex, France

<sup>6</sup>Department of Earth & Atmospheric Sciences, Purdue University, West Lafayette, IN 47907-1397, USA

Accepted 2006 August 25. Received 2006 August 25; in original form 2005 May 11

## SUMMARY

We present a comparison of the vertical displacement monitored by independent techniques at the geodetic observatory of Grasse (France). Both Satellite Laser Ranging and Global Positioning System (GPS) vertical position time-series over the period 1998–2003 show a prominent annual signal with a magnitude of 5–6 mm and reaching a maximum every year in July. Results from 14 absolute gravity measurements are also discussed. We investigate the possible origin of the observed signal by comparing it with predictions from various local and regional contributions. GPS results from a local network indicate that the periodic annual elastic deformation of the ~1270 m high karstic plateau due to local water storage loading does not exceed 1–2 mm. In contrast, a combination of global model prediction for atmospheric and hydrological loading explains more than 70 per cent of the annual and semi-annual observed signals.

**Key words:** crustal deformation, geodynamics, Global Positioning System (GPS), gravity, satellite geodesy, Satellite Laser Ranging (SLR).

## 1 INTRODUCTION

Precisely monitoring the temporal variations of the vertical position of geodetic stations is becoming more and more important for studying tectonic crustal deformation, glacial isostatic adjustment (GIA), sea-level changes, mass loading effects (atmospheric, oceanic, or hydrological) and for terrestrial reference frame realization. The continuous mass redistribution of atmosphere and water (ocean, continental water such as surface and ground water, snow and soil moisture) induces time variations in the gravity field and elastic deformations of the solid earth, primarily in the radial direction. In the past years, these loading phenomena have been recognized as having a major contribution to the Earth's surface vertical motion and the IERS (International Earth Rotation and Reference System Service) recently established a Special Bureau for Loading (SBL) to provide consistent and reliable models of surface mass loading effects (van Dam *et al.* 2002). Accurate monitoring of geodetic height changes allows us to (1) investigate geophysical processes and (2) to validate and improve loading models. Moreover, the study of the temporal stability of the geodetic sites is of great importance for the new representation of the terrestrial reference frame. Indeed, up to

now, reference frame realizations are based on set of reference sites having a simple linear time evolution (Altamimi *et al.* 2002) that do not correctly describe the true site motion.

The accuracy achieved by geodetic techniques now enables us to detect new deformation modes of the Earth (Blewitt *et al.* 2001) and to monitor ground deformations and signals related to global, regional and local environmental effects. Unfortunately, vertical motions of the Earth's crust are usually smaller than horizontal ones. In addition, the vertical positions of geodetic stations are usually less precisely determined than their horizontal components. The main reason is the difficulty to accurately model the propagation of the electromagnetic waves through the atmosphere, which directly contaminate the vertical position estimates. However, significant progress has been made in the last years for all geodetic positioning techniques—Satellite Laser Ranging (SLR), Global Positioning System (GPS), and Doppler Orbitography and Radiopositioning Integrated by Satellite (DORIS)—in terms of their technical features (e.g. better antenna phase centre calibration, Rothacher & Mader 2003) as well as improved data processing techniques (models of satellite, of orbit perturbation, tropospheric zenith delay models, of the Earth . . .). As a consequence of these advancements, shorter

observation spans are required to derive an accurate estimate of the vertical component, thus, allowing us to better monitor geodynamic phenomena over a wide range of frequencies. Among the geodetic techniques, the SLR technique is well suited to accurately determine the vertical component (Degnan 1993). Indeed, the SLR technique offers the advantage of being based on simple and unambiguous range observables, which are insensitive to the ionosphere and less sensitive to the propagation delays introduced by the wet troposphere. However, time-dependent displacements of stations usually have magnitude close to the accuracy of each individual technique, and it still remains a challenge to separate the true geophysical motion from possible artefacts inherent to each measurement system. Comparison of different techniques is, therefore, required to detect any systematic effect induced by an individual technique and extract reliably the true geophysical signal.

The OCA (Observatoire de la Côte d'Azur) fundamental geodetic station is located at Grasse (France) in the southern Western Alps on a ~1270 m high karstic plateau. It is one of the few geodetic observatories operating several collocated space geodetic techniques continuously and offering long time-series. Moreover, absolute gravity (AG) measurements have been performed there regularly since 1998. The purpose of this study is to monitor the vertical displacements of the Grasse observatory. We take advantage of the availability of three independent geodetic monitoring techniques (SLR, GPS and AG) which are collocated there and whose observations span the 1998–2003 period. We attempt to understand the origin of the seasonal signals observed in the geodetic measurements. Ultimately, this will allow us to improve the vertical reference frame and to check the reliability of the vertical reference. The study of the stability of this reference point is of great importance for all the geodetic communities and for all the scientific applications using the terrestrial reference frame. Moreover, comparing different space and ground-based collocated geodetic techniques enables one to understand the possible bias affecting each technique and to extract with reliability the geodynamical signal fully exploiting the potential of each individual technique.

The data and the methodology used for the time-series processing are first summarized. The results are then shown and discussed, paying particular attention to the interpretation of the time-series in terms of geophysical origin of the annual and semi-annual signals.

## 2 DATA SETS

### 2.1 Satellite Laser Ranging time-series

The 5 yr of SLR positioning time-series are computed from tracking data acquired on the LAGEOS-1 and LAGEOS-2 satellites. Though the international SLR network tracks a large diversity of satellites, precise laser station coordinates are almost exclusively based on LAGEOS satellite data. Indeed, their high altitude (6000 km) gives them a particular role for the station positioning determination thanks to their quite stable trajectories and high precision orbit computation.

Our analysis is based on a semi-dynamic approach. In the first step, we computed global 10 d arcs of reference orbits with the GINS software (CNES, France) using the dynamical equations of the satellite movement. In a second step, we used a short-arc method to estimate empirical local geometrical correction of these orbits. To ensure the quality of these orbit computations, we only used data from a subnetwork composed of a representative subset of 11 SLR stations (see Fig. 1a). These fiducial stations

were selected for their high accuracy according to the quarterly reports provided by the ILRS (International Laser Ranging Service, <http://ilrs.gsfc.nasa.gov/>). Moreover, this subset is a realization of a good geometry for SLR over the Earth's surface (three in Europe, three in the USA, two in Australia, one in South Africa, one at Hawaii and one in South America; see Fig. 1a). The Grasse OCA station data are not included in the orbit determination. The global LAGEOS orbit precision (mean rms) is between 12 and 23 mm for all the 10 d arcs used in this study. The mean residual over the whole period for the Grasse station is 4.9 mm for the LAGEOS-1 satellite and 6.4 mm for the LAGEOS-2 satellite, and so 5.7 mm for both satellites. We then use the reference orbits to determine the Grasse station coordinates every 30 d. According to our tests, 30 d is found to be the best trade-off ensuring a sufficient number of data to allow us to decorrelate each coordinate component while maintaining the best temporal resolution. The coordinate estimation is performed through a classical least-squares method from combined normal equations of the two LAGEOS satellites. We compute coordinate residuals with respect to the ITRF2000 (Altamimi *et al.* 2002) reference frame used as the *a priori* solution. The models included in the analysis are the GRIM5-S1 (Biancale *et al.* 2000) gravity field and the IERS96 Conventions (McCarthy 1996) for solid earth tides (elastic case) and Wahr (1985) solid-earth pole tide model. It should be emphasized that no loading effects have been included in the SLR analysis.

These time-series span the 1997 October–2002 October period. The typical formal uncertainty ( $1\sigma$ ) of the vertical component is 2 mm.

### 2.2 Global Positioning System time-series

To compute the GPS time-series, we used the global weekly combined position solutions provided by CODE (Centre for Orbit Determination in Europe) analysis centre in the frame of the IGS (International GPS Service). Details regarding the data processing strategy used are given in the CODE analysis reports to the International Service for Geodynamics to which the reader is referred (Rothacher *et al.* 1998); (Hugentobler *et al.* 1999, 2000, 2002). The network analysed is shown in Fig. 1(b). Zenithal delay corrections are estimated every 2 hr using the wet-Niell mapping function (Niell 1996). One N–S and one E–W horizontal delay parameter per day for each station is solved for. No constraint is applied on either the zenith or the gradient parameters. Solid earth displacement corrections are applied using the complete model from the IERS Conventions 1996 (McCarthy 1996) and ocean tides effects are corrected according to the model of Scherneck (1991). As with the SLR data processing, atmospheric, non-tidal ocean and hydrological loading are not taken into account in the GPS analysis.

We include solutions spanning the period 1998 January–2003 September. We first remove the reference frame constraints applied to the weekly CODE solution and then we combine the unconstrained weekly solution using the CatRef software (Altamimi *et al.* 2002). Simultaneously, we solve for any offset in the time-series. Minimal constraints on the global network are applied in order to express our time-series in the ITRF2000 (Nocquet & Calais 2003). The typical standard deviation on the vertical component is 4 mm ( $1\sigma$  level) while the short-term repeatability (calculated over 7 d) is 6 mm. We chose to use a global solution rather than a regional solution for several reasons: (1) Using a regional network would imply the use of a regional implementation of the reference frame. Since the ITRF realizations so far only include a linear

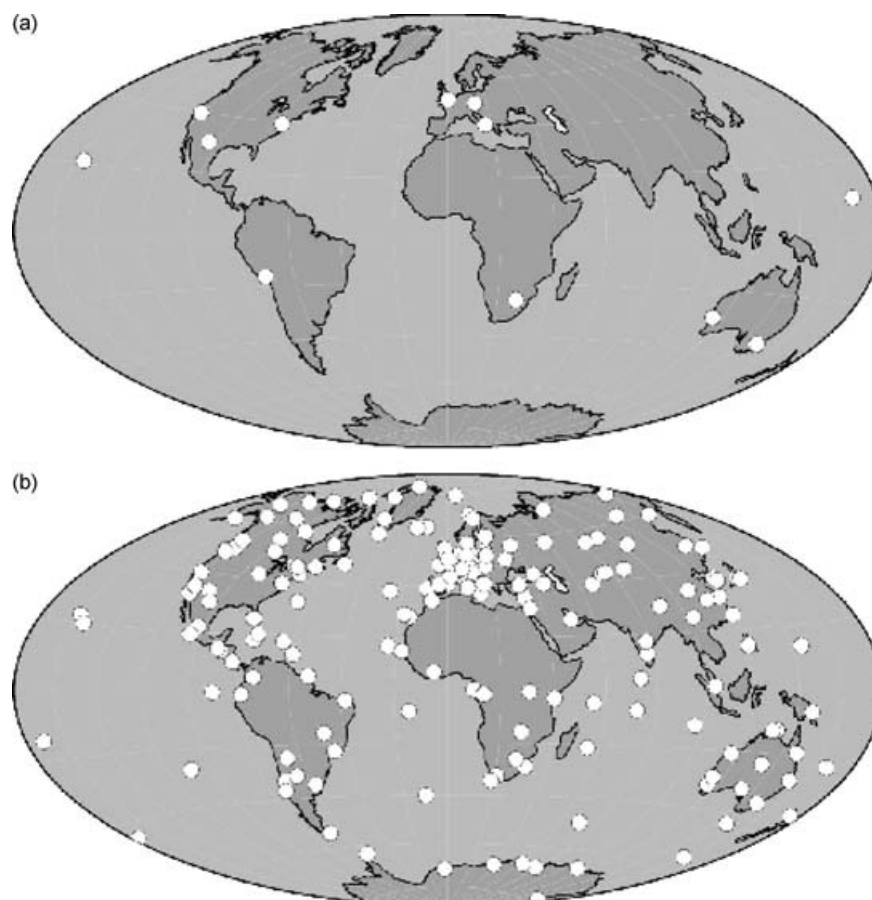


**Figure 1.** Networks used in the positioning time-series computation for (a) SLR and (b) GPS.

model (position given at a reference epoch and the associate velocity), the reference frame implementation would absorb any large-scale motion. A regional implementation is, therefore, equivalent to a regional spatial filter (Williams *et al.* 2004). (2) Tregoning & van Dam (2005) have recently shown that a reference frame implementation through seven parameters transformation could induce important biases in the vertical for regional networks. (3) Vertical SLR position time-series are calculated in a global reference frame implemented through the orbits. Any rigorous comparison of the GPS and SLR techniques requires a common reference frame.

### 2.3 Absolute gravity measurements

Since 1998, 14 campaigns of AG measurements have been performed at the OCA using FG5 absolute gravimeters operated by two different teams: FG5#206 for the EOOST (Ecole et Observatoire des Sciences de la Terre), Strasbourg (France) and FG5#202 for the Royal Observatory of Belgium (ROB). Incidentally, the Grasse observatory is one of the French reference points used to check the calibration of relative spring gravimeters.

The FG5 AG measurements usually consist of one set per hour with the average of several sets (average of 100 drops of a free-falling corner cube), usually 12 to 48 in 1 or 2 d, providing the epoch 'gravity value'.

The instrumental accuracy of the FG5 is about 1–2  $\mu\text{Gal}$  as reported by the manufacturer (Niebauer *et al.* 1995). Even though the FG5 is an absolute instrument, occasional offsets due to miscalibra-

tion of the clock, to the barometer, etc. have been observed. Thus, the two FG5s involved in this study have been regularly compared in different sites and the differences accounted for (Van Camp *et al.* 2003). As a result of these comparisons, only one series of measurements done with the FG5#206 (EOST) needed to be adjusted: an offset of 4.35  $\mu\text{Gal}$  for the 2002 February campaign.

The final gravity value is obtained after applying corrections for Earth tides, ocean loading and polar-motion effects using the proprietary g-software developed by Micro-g (Micro-g Solutions Inc. 2004). Unlike positioning techniques, gravity is affected by the surface masses in two ways. First, gravity changes due to the attraction of the excess mass. Second, gravity changes as a result of the surface deformation. In this study, no correction for the atmospheric effect was applied. This allows us to directly compare the surface deformations with the gravity changes.

## 3 RESULTS

Fig. 2 shows the different time-series for the three different techniques from 1997.6 to 2003.7. The GPS time-series are corrected for a slope estimated over the whole time-series. Since our solutions are expressed in the ITRF2000, our vertical velocities are relative to the ITRF2000 origin. The ITRF2000 origin is defined by imposing a condition of no translation and no translation rate relatively to the weighted average of five SLR solutions included in the ITRF2000 calculation (Altamimi *et al.* 2002). As a consequence, the ITRF2000 origin corresponds to a position and rate of position change of the centre of mass of the whole Earth (solid earth, ocean,

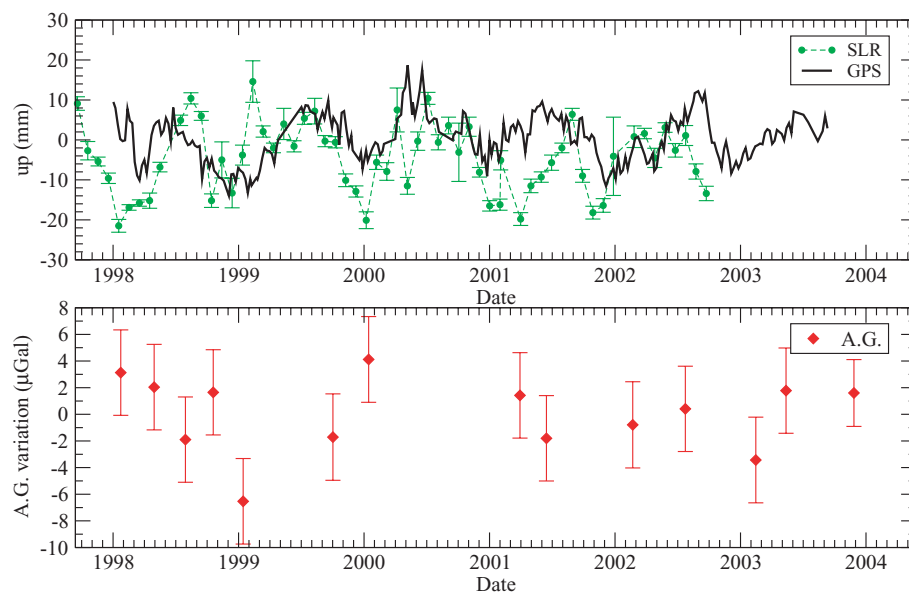


**Figure 2.** SLR, GPS, and AG time-series at the OCA Grasse observatory (France). The SLR (dashed line) and GPS (solid line) represent the vertical positioning component given in millimetres relatively to ITRF2000 coordinates. The AG values (diamonds) are given in  $\mu\text{Gal}$  relatively to the mean  $g$  value of the 14 campaigns. The AG and SLR error bars represent 1 standard deviation.

atmosphere) averaged over the period included in the five SLR solutions in the ITRF2000 (i.e.  $\sim 20$  yr of measurements). We note that the vertical SLR position residual with respect to ITRF2000 over the whole period is  $-4.6$  mm. This bias corresponds to the station range bias. Using a collocation experiment between three independent SLR stations performed at the Grasse observatory in 2001, this bias has been attributed to a range bias of 5 mm on LAGEOS observations (Nicolas *et al.* 2002). This correction has been applied to obtain the results in Fig. 2. Discrepancies relative to the ITRF2000 values are found to be very small and within the velocity uncertainty: the difference in velocity is  $-0.3 \pm 0.8$  mm yr $^{-1}$  for our SLR solution and  $0.4 \pm 0.2$  mm yr $^{-1}$  for the GPS. The  $g$  variation values are given relatively to the mean value of  $g$  on the entire period considered in this study. This  $g$  mean value is  $980215549.2 \pm 12.6$   $\mu\text{Gal}$ .

Both SLR and GPS time-series of the vertical component show significant seasonal variations. The signal has a mean peak to peak amplitude of 25 mm for SLR and 20 mm for GPS, and varies slightly in amplitude from year to year.

To better quantify the periodic signals included in our time-series, we used Period98 (Sperl 1998), an algorithm that searches for sinusoidal patterns within a time-series containing gaps. This package uses Fourier analysis and performs simultaneously multiple-least-squares algorithms. The results of this analysis indicate that the annual term dominates the signal for both time-series. Its magnitude is 5.5 mm for the GPS time-series and 6.1 mm for SLR which corresponds to an 11 to 12 mm peak to peak signal. This is in agreement with the 1–2 cm vertical displacements occurring in the Northern Hemisphere due to atmospheric pressure loading (van Dam & Wahr 1987). The maximum of the annual signal is observed in July for both GPS and SLR.

Similar amplitude annual signals in the geodetic height component and  $g$  variations are observed at other sites, for example, the Po plain (Zerbini *et al.* 2001); (Richter *et al.* 2004), in the lower and upper Rhine Graben (Francis *et al.* 2004); (Amalvict *et al.* 2004), in west Canada (Lambert *et al.* 2002). Global analyses of the annual

signal have been provided by Mangiarotti *et al.* (2001) and Dong *et al.* (2002).

A semi-annual component of the signal can also be extracted from both SLR and GPS time-series with amplitudes of 2.8 and 1.4 mm, respectively, which correspond to 5.6 and 2.8 mm peak to peak signals.

Similar periodic signals exist in the horizontal components but their magnitudes are smaller ( $\sim 2$  mm) and not well resolved given the accuracy of our data. Moreover, the AG measurements cannot provide a determination of these horizontal movements. Hence, we focus only on the vertical deformations.

No clear annual signal is observed in the AG time-series. Fitting an annual term to the AG time-series provides an amplitude of 1.4  $\mu\text{Gal}$ . The Period98 algorithm also indicates a second principal term with a period of 204 d and a magnitude of 2.6  $\mu\text{Gal}$ . However, the AG measurements were performed episodically and are limited to short time intervals. Because of this irregular and sparse time sampling, we do not put much confidence in these results.

## 4 DISCUSSION

### 4.1 Impact of the Newtonian effect on gravity measurements

The AG signal is not simple and its comparison with the height variations measured by SLR and GPS is not direct. If we take for the gravity gradient a value of  $-0.2$   $\mu\text{Gal mm}^{-1}$ , which is the so-called Bouguer corrected free air gradient (see e.g. Ekman & Mäkinen 1996), to convert gravity variations into vertical surface displacements, the possible annual AG signal amplitude is equivalent to 6.9 mm which is of the same order of magnitude as the GPS and SLR signals. If gravity is monitored with a better temporal resolution in the future, a possible significant discrepancy with the positioning time-series may appear as gravity contribution of the water level changes under the observatory must be expected.



The loading phenomena modify the surface gravity through direct and indirect effects. The first one is the direct gravitational attraction by the atmospheric or water masses and is also called the Newtonian effect. Gravity measurements are indeed affected for instance by vertical air mass exchanges, which cannot be observed by ground pressure measurements alone. The vertical variations in the atmospheric density change the attraction force of the air masses on the gravimeter. These direct effects of mass displacements (i.e. atmospheric masses, snow . . .) are not measurable at LAGEOS and GPS satellite altitudes (about 6000 and 20 200 km, respectively) in terms of orbitography. The second effect, called the indirect or elastic effect, is linked to the global deformation of the Earth's crust due to the planet's elasticity (see e.g. Hinderer *et al.* 1991). It is the elastogravitational effect, which can be modelled with the Green's functions (Farrell 1972). This elastic contribution induces a deformation of the Earth (in particular radially) and the mass redistribution also changes the Earth's gravity field. Therefore, the gravity effect induced by global pressure variations is the sum of these three effects (a Newtonian attraction, the surface deformation induced by loading, and gravity field variations) (Boy *et al.* 2002) whereas the SLR and GPS techniques are only sensitive to the atmospheric pressure induced ground deformations. Thus, the AG signal cannot be directly compared to the positioning time-series.

Generally, AG measurements are converted into vertical displacements with a constant gradient. The ratio initially used at the OCA was  $-0.2 \mu\text{Gal mm}^{-1}$ . However, a simple transfer function between gravity and height variation cannot be applied since it is only a mean model, which does not take the frequency dependence of the admittance into account. Thus, converting gravity into vertical displacement in case of loading effects can be misleading and we preferred not to apply any conversion of AG into vertical displacements in this study. We computed the full loading effects both in vertical displacement and gravity using the appropriate Green's functions.

Another possible explanation for this discrepancy is the contribution to gravity measurements of local ground water mass variations stored in the karsts. The observed AG variations (up to  $8.8 \mu\text{Gal}$  min-max) would be explained for instance by a 5 m water level variation in a 1 km radius cylindrical ground water table located at 800 m depth, with 10 per cent porosity of the karst. The local character of this load would lead to negligible changes in deformation (Llubes *et al.* 2004). This solution is realistic but there is not enough information on the ground water table (depth, size . . .) located under the observatory to conclude since underground structures with permeable and impermeable layers are not well known in this area (Gilli, private communication, 2004).

## 4.2 Impact of time-series processing strategy

Different processing software and data analysis strategies may produce different results. In order to assess the potential effect of our chosen analysis strategy on the annual signal estimate, we have made several comparisons. First, we compare our GPS time-series with a recent global analysis made by Nocquet *et al.* (2006) using the GAMIT/GLOBK software rel. 10.2 (King & Bock 2005). The strategy uses a three-step approach described in Feigl *et al.* (1993) and Dong *et al.* (1998). IGS final orbits are used in a relaxed mode (satellite state vectors are estimated), and elevation-dependent antenna phase-centre models are applied following the tables recommended by the IGS to produce a daily loosely constrained solution. Tropospheric zenith delays and horizontal gradients are estimated using the Niell mapping function every 2 hr. Solid earth and polar tide cor-

rections following the IERS Conventions 2003 (McCarthy & Petit 2004), and ocean loading corrections using the CSR4.0 ocean tide model (Eanes & Schuler 1999) are taken into account. Reference frame constraints are applied at the third step using generalized constraints (Dong *et al.* 1998) while estimating a six-parameter transformation (three translations, three rotations, no scale factor applied).

While differences are noted in the weekly coordinates computed with the two processing strategies (rms = 8 mm), the magnitude of the annual signal is consistent with our solution (6.0 mm). The phase is however shifted by 2 months with a minimum observed usually during the autumn. We conclude that the magnitude of the annual periodic signal observed in Grasse is not sensitive to the strategy or software used. However, a possible shift in the phase of 2–3 months should be considered when comparing the observations to surface displacements predicted using the surface mass models.

We also studied the influence of the SLR time-series computation strategy. For this, we compared our time-series with the ones provided by independent analyses performed at the OCA (Coulot 2005) and by the ASI (Agenzia Spaziale Italiana) SLR centre available on the ILRS website (<http://ilrs.gsfc.nasa.gov/>). The first time-series was computed from the same reference orbits but each 10 d (instead of 30 d) with a correction of the residual orbit errors with an independent software. At Grasse, the impact of the residual orbit error on the vertical positioning is only 1.3 mm (the average of all the arcs obtained during the period considered). The correlation between these two solutions is 0.78 with a regression coefficient (slope) of  $0.86 \pm 0.09$  when expressing one solution with respect to the other. The annual term amplitude difference between these two time-series is 0.1 mm and displays a phase shift of 20 d. For the semi-annual term, the amplitude difference is lower than 1 mm and also with a phase shift of 20 d. This phase shift is not surprising when we remind that one of the two solutions has a time sampling of 30 d. The ASI time-series is expressed in the ITRF2000 reference frame using the CatRef software as was done for the GPS solutions. For this time-series, the 3-D coordinates are computed each 7 d simultaneously with daily EOP (Earth Orientation Parameters) solutions. The annual term of the vertical component of this time-series shows a difference of less than 1 mm in amplitude and a phase difference of about 2 months relative to the SLR time-series used in this study. These discrepancies most likely arise due to the simultaneous computation of 3-D station coordinates and EOP, with a time sampling which does not allow a good decorrelation between all the adjusted parameters. Nevertheless, even if there are differences between the different time-series, the robustness of the annual signal is confirmed by the agreement from various time-series investigated.

Both our SLR and GPS time-series refer to the origin of the ITRF2000. The ITRF2000 origin is determined through a weighted average of the SLR solutions included in the ITRF2000 calculation. It, therefore, realizes a centre of mass (solid earth + its fluid envelopes) averaged over the time period spanned by SLR data included in the ITRF2000 (1980–2000). As a consequence, any short-term motion of the geocentre relative to the ITRF2000 origin would theoretically leak into our height estimate as explained by Tregoning & van Dam (2005). However, large uncertainties exist both on models/estimates of geocentre motion (see for instance Chen *et al.* 1999, for a comparison of model and geodetic estimates). We can simply test whether the impact of geocentre motion on our time-series is significant by looking at a common mode translation for sites located over Europe. For SLR data, a similar seasonal signal is found at Graz (Austria), but not in Wettzell (Germany). For GPS data, height time-series become decorrelated as the distance between the sites

increases, suggesting again that most of the signal has a regional origin rather than a global one.

### 4.3 Local or regional effects?

The annual period observed independently in both GPS and SLR time-series suggests that it results from a true geophysical process rather than from a geodetic processing related origin. In the following, we therefore test the contribution of different possible geophysical processes to the annual periodic signal. We first start by investigating possible local effects. The Grasse observatory is located on a  $\sim 1270$  m karstic plateau that might respond elastically to water storage changes. In order to quantify possible local deformation contributions to our time-series, we use the local permanent GPS sites available around the Grasse observatory (REGAL, Calais *et al.* 2000). If local deformation of the karstic plateau is the major contribution to the observed signal, then local (20–100 km) 3-D GPS baselines including GRAS should clearly detect it. Moreover, assuming that none of the surrounding sites are affected by similar effects, the signal should be consistent for all the baselines and the pattern of the GRAS signal should be enhanced by simply stacking the baseline time-series. Alternatively, if the signal in GRAS is representative of a more regional displacement, then the short baselines ( $< 150$  km) should show a random signal which would reflect the noise of the measurements.

We use four GPS sites (MICH, MARS, SOPH, GENO) located in different tectonic areas with distances ranging between 20 and 100 km from GRAS (Fig. 3a). We fix the coordinates of the four sites and look at the height time-series of GRAS relative to those sites and stack them. The stacked time-series clearly shows a consistently common signal for the four baselines, a 4 mm annual signal with a maximum in April when the water storage in the karstic plateau is expected to reach a maximum (Fig. 3b). However, 4 mm in the stacking of the four time-series corresponds to an averaged annual signal of only 1 mm of magnitude on any individual baseline with a maximum occurring 3 to 5 months before the maximum observed in the global SLR and GPS time-series. We conclude that local effects contribute only marginally (15 per cent) to the observed annual signal. As a consequence, the main part of the observed signal originates from a regional to continent scale loading effect that can be investigated through comparisons to loading models.

### 4.4 Comparison with the loading models

Changes of mass distribution in the atmosphere, in the ocean circulation and tides, and in the continental water mass (snow, ice, soil moisture, rainfall, ground water level) induce surface deformation. The cumulated vertical Earth surface deformation due to these loading effects can reach a few centimetres.

In general, the largest effect in magnitude is the atmospheric loading, which induces Earth deformations due to variations in the horizontal and vertical distributions of atmospheric mass (van Dam & Wahr 1998). Atmospheric loading mainly induces vertical surface displacements and changes in gravity at the displaced surface through a pressure loading at the surface and through attraction of the atmospheric mass. Atmospheric pressure loading can cause peak to peak displacements of the Earth's surface as large as 10 to 25 mm (Rabbel & Zschau 1985), (van Dam *et al.* 1994), (van Dam & Herring 1994). Bock *et al.* (2005) illustrate the atmospheric loading effect on SLR station positioning. The main periods of the atmospheric loading effect are seasonal. The largest pressure variations,

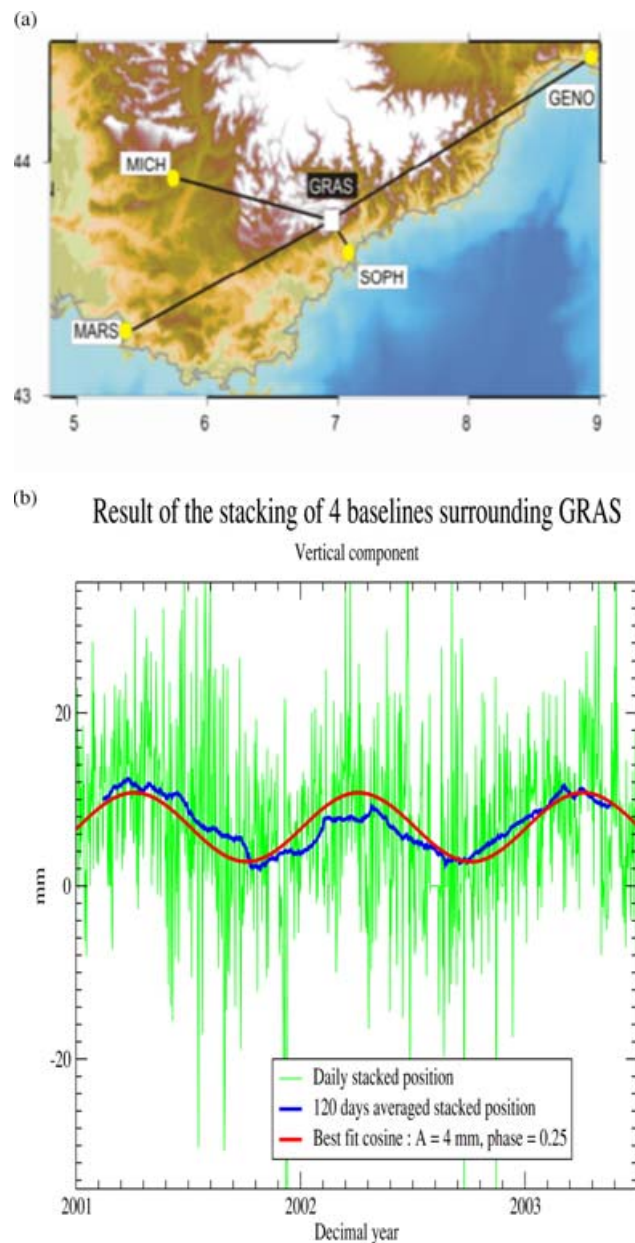


**Figure 3.** (a) The Grasse GPS/SLR/AG station and the other surrounding REGAL stations (Western Alps, Calais *et al.* 2000). (b) Stacking of the vertical component of the 4 baselines including Grasse and the surrounding 4 sites from the REGAL solution. The solid line shows the annual signal with magnitude of 4 mm, corresponding to 1 mm at Grasse only.

however, are linked to storms, but do not contribute appreciably to the seasonal signal because of their short lifetime which is usually less than 10 d (van Dam & Wahr 1987) and tend to average to zero in a daily time-series. On the other hand, these storms can disturb specific AG measurements significantly (several  $\mu\text{Gal}$ ) because the AG measurements are discontinuous in time.

We compared the observed vertical positioning and AG time-series with the predicted deformations and gravity changes derived from global atmospheric, ocean, and hydrological loading models. The time-series due to atmospheric loading were computed from the ECMWF (European Center for Medium-Range Weather Forecast) pressure field each 6 hr from 1992 to 2003 using the technique described in van Dam *et al.* (2002). The 3-D site coordinates are

computed relatively to the global earth centre of mass. From this model, the annual signal for GRAS has a magnitude of 1–2.5 mm.

The tidal ocean loading time-series was computed from the FES99 model (Lefèvre *et al.* 2002) by temporal addition of the effects of the eight main waves (M2, S2, K1, O1, N2, P1, K2, Q1) each hour from 1998 to 2004 (Llubes, private communication, 2004). However, at Grasse the tidal ocean loading effect is negligible since it is located on the French coast on the Mediterranean Sea. The non-tidal oceanic contribution is based on bottom pressure outputs from the ECCO (Estimating the Circulation and Climate of the Ocean) general circulation model (<http://www.ecco-group.org/>). According to Llubes (private communication, 2004) and to Dong *et al.* (2002), the cumulative effect of tidal and non-tidal ocean loading is at the level of 1 mm for Grasse for the annual and semi-annual signals on the vertical component and does not significantly contribute to the observed signal.

Finally, we used displacement and gravity (Newtonian and indirect elastic effect) time-series using the hydrological models proposed by Milly & Shmakin (2002) and by Rodell *et al.* (2004). As before, these computations are performed in a reference frame linked to the global earth centre of mass. The first hydrological model has a spatial resolution of  $1^\circ$  and a temporal sampling of

1 month from 1980 to 2003. The second also has a  $1^\circ$  spatial resolution, but presents the advantage of a 3 hr temporal resolution. Unfortunately, this latter time-series is only available for 2002 and 2003. For the two years (2002 and 2003) where the two models prediction can be compared, the seasonal component shows good agreement in phase between the two models (Boy & Hinderer 2006). The magnitude however differs by 10–20 per cent. The amplitude of the seasonal hydrological loading is estimated at 2–3 mm in vertical displacement and about  $3 \mu\text{Gal}$  in gravity variations for the annual period (Fig. 4).

Figs 5 and 6 show the comparison between the observed time-series and the time-series computed from the different loading models introduced above. The overall agreement between the observations and the predicted vertical deformations is quite good, in particular for the SLR and GPS solutions. Figs 7(a) and (b) show the discrete Fourier transform (DFT) of the SLR and GPS vertical positioning time-series. The signal analysis indicates that the cumulative effect of the different contributions (ECMWF, FES99, Milly & Shmakin 2002) explains the bulk of the signal. The correlation coefficient between SLR and the surface displacements predicted from the cumulative mass model is 0.49, with a regression coefficient (slope) of  $1.24 \pm 0.30$ . The correlation coefficient between

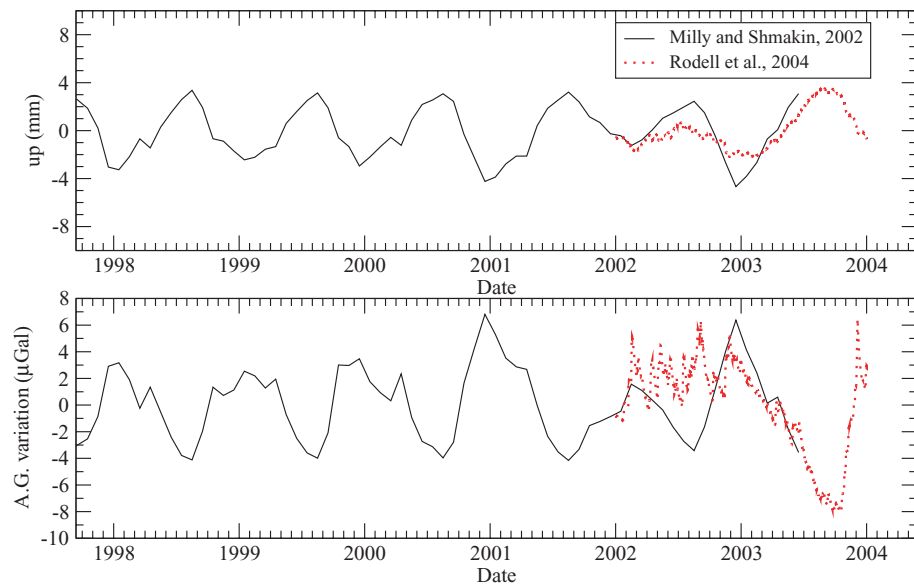


**Figure 4.** Hydrological loading models considered in this study: Milly & Shmakin (2002) (solid line) and Rodell *et al.* (2004) (dashed line) for vertical displacement (in millimetres) and gravity variations (in  $\mu\text{Gal}$ s).

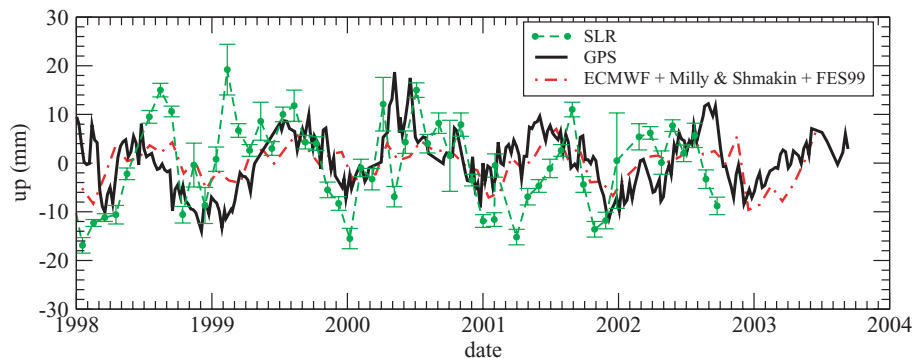


**Figure 5.** Comparison of the vertical displacement time-series between the observations of SLR (dashed line) and of GPS (solid line) and the addition of atmospheric (ECMWF), oceanic (FES99), and hydrological (Milly & Shmakin 2002; Rodell *et al.* 2004) loading models (dotted line).



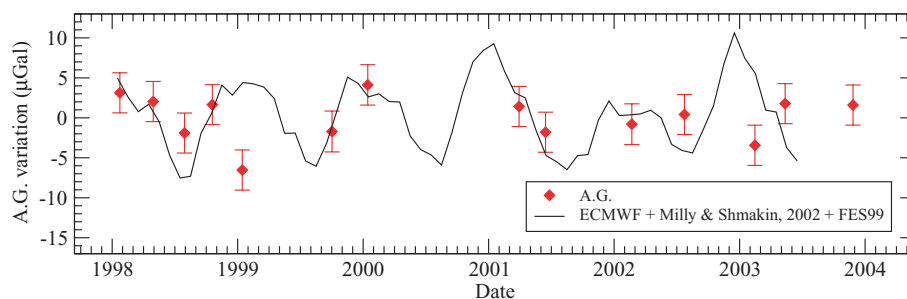


**Figure 6.** Comparison of the AG measurements (diamonds) with the cumulative effect of atmospheric (ECMWF), oceanic (FES99), and hydrological (Milly & Shmakin 2002) loading models (solid line). The AG error bars represent 1 standard deviation.

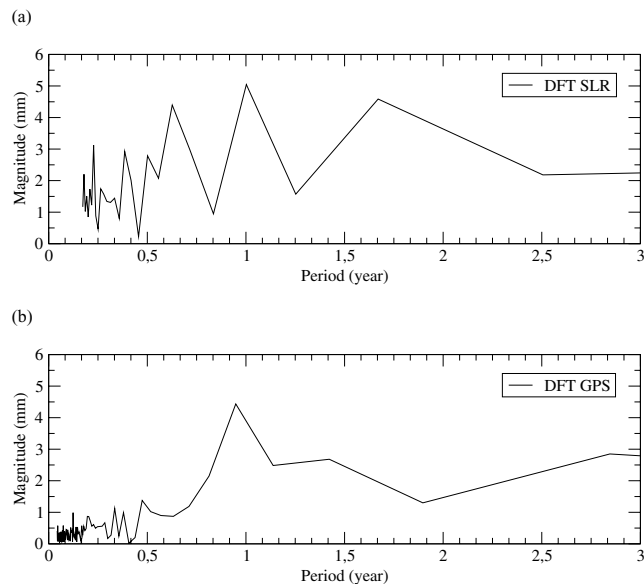


**Figure 7.** Magnitude (in millimetres) versus period (in years) from the DFT analysis of the vertical positioning time-series for (a) SLR and (b) GPS.

GPS and the models is 0.46 and the regression coefficient (slope) is  $0.72 \pm 0.09$ . To estimate the part of the signal explained by the cumulative effect of the loading models, we computed the DFT of the difference between the observation time-series (SLR and GPS) and the predicted time-series. For SLR 75 per cent of the annual term and 70 per cent of the semi-annual terms are explained. For GPS, the deformation from the environmental mass models explains 65 per cent of the annual term and 100 per cent of the semi-annual term. If we consider the Rodell *et al.* (2004) hydrological loading model, instead of the Milly & Shmakin (2002), the DFT analysis shows that almost the entire annual and semi-annual terms are explained for both SLR and GPS for the time spans that the model data are available. Concerning the AG time-series, we found a correlation coefficient of 0.72 with the models and a regression coefficient of  $0.41 \pm 0.13$  if we remove the 5th point (beginning of 1999). This data editing is justified as there was a storm during this AG measurement campaign.

In vertical displacement, the 5–6 mm annual signal can be finally separated into the following contributions:

- (i) 1–2.5 mm from atmospheric loading,
- (ii) 1 mm from tidal and non-tidal ocean loading and
- (iii) 2–3 mm from hydrological loading.

The agreement between the observed and the modelled seasonal fluctuations is fair, as well in height as in gravity time-series. Even if the main part of the signal is explained by the cumulative effect of atmospheric, hydrological, and ocean-loading phenomena computed from global models, a residual signal remains. The effect of long-wavelength seasonal variability in continental water storage on vertical crustal positions, modelled by van Dam *et al.* (2001), can reach up to 30 mm with a primarily annual periodicity. Thus, improved models of continental water storage and the loading effects of snow and ice are to be taken into account to explain the integrity of the observed signal.

We showed that the main origin of the signal is at a regional scale. Nevertheless, a part of the residual signal at higher frequencies may still be caused by a local hydrology effect. A study performed from 1997 September to 1999 May indicated that there is no correlation between the gravity variations and the rainfall (Gilli 2002). To better understand the local hydrology, a study is currently being performed to investigate water circulation through wet air transport as well as its condensation and evaporation measurements in the underground galleries and inside the rocks themselves (Walch, private communication, 2004). Indeed, considering the high porosity (10–15 per cent) of the karsts at Grasse, the percolation may present seasonal variations linked to climatic and atmospheric seasonal variations. Then, local effects could be due to the karsts where the water circulation could (strongly) affect the gravity value. However, the vertical deformation due to the loading of the karstic reservoirs is expected to be lower than 1 mm.

Another source of discrepancy could be the impact of the inverted barometer (IB) or non-IB hypothesis in the atmospheric loading model since the Grasse observatory is very close to the Mediterranean Sea. Indeed, a site displacement linked to atmospheric loading depends also on the site distance with respect to the coast. In the non-IB case, the oceanic response is the same as for the solid earth and all pressure effects are fully transmitted to the Earth whereas in the IB case, the pressure variations are compensated by the variations of sea depth, and there is no net pressure variation on the seafloor. However, the IB and non-IB ocean models cannot take into account the atmosphere, solid earth and ocean interactions. MacMillan & Gipson (1994) and Boy *et al.* (1998) used a model of the non-global static ocean response, which allows for a better approximation of the atmosphere–ocean–earth interactions, by a simultaneous resolution of the equilibrium equations of the non-global ocean and the elastogravitational equations of the solid earth. For van Dam *et al.* (1997), the oceans respond in order to compensate air pressure changes by sea-depth variations, and with a no-net pressure change on the deformed seafloor due to pressure field over the oceans (like in IB, but there are additional effects due to the redistribution of the water masses to the continental pressure loading). Nevertheless, this

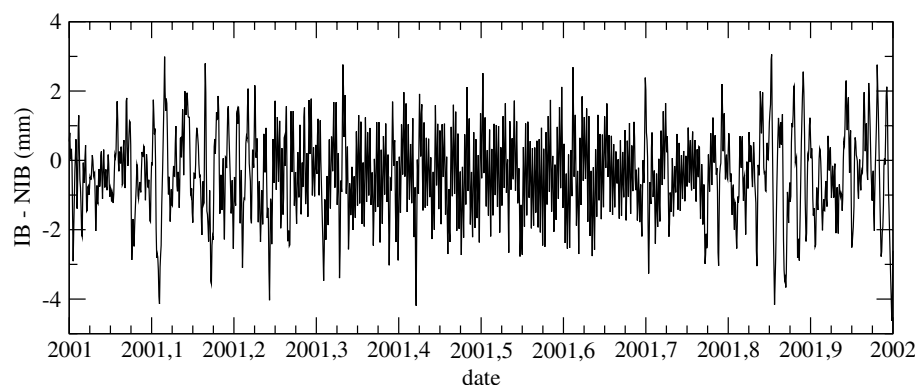


**Figure 8.** Difference of vertical displacement due to the atmospheric loading computed from ECMWF data with and without the IB hypothesis (in millimetres) at Grasse for 2001.

impact should be very small (de Viron *et al.* 2004). We studied the impact of the IB hypothesis for the Mediterranean Sea in the atmospheric loading effect computation. Fig. 8 illustrates the results of this test for 2001. The difference of the predicted vertical displacement is quite small (mean lower than 0.5 mm, standard deviation of 1 mm). So, we confirm that the impact of IB or non-IB hypothesis for the atmospheric loading model is quite small at Grasse.

However, above all, we think that the main part of the residual signal is due to the fact that the global loading models used in this study do not take into account the local characteristics of the Grasse observatory, and in particular the local topography for a better estimate of the nearby attraction effects. Indeed, the Grasse observatory is located about 20 km from the Mediterranean Sea in the southern extensions of the French Alps, where the topography rises from 0 m to over 3000 m over a distance of only 200 km. Indeed, considering the local topography could have a non-negligible impact, particularly for the atmospheric and hydrological loading effects. For instance, it highly reduces the rms of the vertical deformation and of the gravity variations computed for atmospheric loading.

## 5 CONCLUSION AND PROSPECTS

By comparing different space and ground-based collocated geodetic techniques, we have been able to extract a reliable geodynamical signal at the OCA geodetic fundamental station. This kind of comparison is of the utmost importance for improving the vertical reference frame. Moreover, the AG being absolute is not network dependent and provides an independent way of measuring the long-term stability at the OCA observatory (Van Camp *et al.* 2005).

Since the signal amplitude is at the subcentimetre level in position and at the few  $\mu\text{Gals}$  level in gravity, the signal is still close to the intrinsic accuracy of SLR, GPS, and AG individual technique. However, SLR and GPS time-series show a consistent annual signal with an amplitude at the centimetre level peak to peak, estimated over a period of 6 yr. This good agreement between the two independent techniques suggests a true physical annual vertical displacement of magnitude of 5 to 6 mm. Analysis of local baselines suggest that possible local effects are of the order of 1 mm and cannot exceed 2 mm. Both Dong *et al.* (2002) and the model used in this study (from the ECMWF data) agree that atmospheric loading could not exceed 1–2.5 mm south of the Western Alps. Tidal and non-tidal ocean loading similarly cannot produce an annual signal higher than 1 mm at Grasse. We conclude that the main contribution to the observed signal is caused by hydrological loading at the regional or continental scale. Indeed global hydrological models do suggest a

2–3 mm possible magnitude (Dong *et al.* 2002); (Milly & Shmakin 2002); (Rodell *et al.* 2004). The cumulative effects of the atmospheric, ocean and especially the hydrological loading effects at the European continental scale could explain more than 70 per cent of the annual and semi-annual observed signals.

Concerning the AG time-series, due to the lack of data, not much confidence can be put in the search for periodic signals. Another problem is the unknown local effects from the water masses in the karsts. The installation of a superconducting gravimeter (SG) would provide a precise and continuous monitoring of gravity variations, while semi-annual AG measurements would control the SG instrumental drift. Another possibility is a permanently available AG measuring once a week or fortnightly. Because of its absoluteness, the AG technique is also very valuable to constrain long-term tectonic deformation. These repeated AG or continuous SG measurements would monitor accurately the local signal linked to the karsts, providing valuable information on ground water variations and on the annual height variations throughout the year.

As the OCA is located on a plateau, it could also be essential to take into account the atmosphere located under the plateau, especially for AG measurements. In the global models, and particularly for the atmospheric loading, the proximity of the sea (south) and of the Alps (north) should be taken into account. We plan to apply hydrological and atmospheric loading models taking into account the local topography particularities of the OCA observatory to better understand the possible contribution to the signal we observe. In particular, we will focus on continental water storage effects on vertical crustal motions, which can reach up to 30 mm (van Dam *et al.* 2001), and on the impact of the local topography on the predicted deformations and gravity variations.

## ACKNOWLEDGMENTS

We thank B. Luck (EOST) who performed the majority of the AG measurements. We are grateful to the OCA laser team for their contribution to LAGEOS-1 and LAGEOS-2 satellite data acquisition. We thank the GPS team for supporting the experiment. We acknowledge the ILRS and the IGS for providing the observations and analysis results used in this study. We are grateful to J.-J. Walch who coordinated the gravity campaigns and who performs geophysical measurements at the Grasse observatory. The authors wish to acknowledge helpful discussions with F. Barlier (OCA), P. Exertier (OCA), F. Mignard (OCA), M. Greff (IPGP), H. Legros (EOST), J. Haase (Purdue University), and E. Gilli (Paris 8 University).

Thanks are also due to D. Coulot (OCA) for his SLR time-series and to ASI SLR team members for their SLR time-series. We thank M. Llubes (CNES) for providing us the time-series of tidal ocean loading. Finally, we acknowledge the anonymous reviewers for their constructive remarks.

## REFERENCES

- Altamimi, Z., Sillard, P. & Boucher, C., 2002. ITRF2000: a new release of the International Terrestrial Reference Frame for Earth science applications, *J. geophys. Res.*, **107**, 2214, doi:10.1029/2001JB000561.
- Amalvict, M., Hinderer, J., Makinen, J., Rosat, S. & Rogister, Y., 2004. Long-term and seasonal gravity changes and their relation to crustal deformation and hydrology, *J. Geodyn.*, **38**, 343–353.
- Biancale, R. et al., 2000. A new global Earth's gravity field model from satellite orbit perturbations: GRIM5-S1, *Geophys. Res. Lett.*, **27**, 3611–3614.
- Blewitt, G., Lavallée, D., Clarke, P. & Nurutdinov, K., 2001. A new global mode of the Earth deformation: seasonal cycle detected, *Science*, **294**, 2342–2345.
- Bock, D., Noomen, R. & Scherneck, H.-G., 2005. Atmospheric pressure loading displacement of SLR stations, *J. Geodyn.*, **39**(3), 247–266.
- Boy, J.-P. & Hinderer, J., 2006. Study of the seasonal gravity signal in superconducting gravimeter data, *J. Geodyn.*, **41**, 227–233, doi:10.1016/j.jog.2005.08.035.
- Boy, J.P., Hinderer, J. & Gegout, P., 1998. Global atmospheric loading and gravity, *Phys. Earth planet. Inter.*, **109**, 161–177.
- Boy, J.P., Gegout, P. & Hinderer, J., 2002. Reduction of surface gravity data from global atmospheric pressure loading, *Geophys. J. Int.*, **149**, 534–545.
- Calais, E. et al., 2000. REGAL: A permanent GPS network in the French Western Alps, Configuration and first results, *C.R. Acad. Sci. Paris*, **331**, 435–442.
- Chen, J.L., Wilson, C.R., Eanes, R.J. & Nerem, R.S., 1999. Geophysical interpretation of observed geocenter variations, *J. geophys. Res.*, **104**(B2), 2683–2690, 10.1029/1998JB900019.
- Coulot, D., 2005. Télémétrie laser sur satellites et combinaison de techniques géodésiques. Contributions aux systèmes de référence terrestres et applications, *PhD thesis*, Observatoire de Paris, 7 juillet 2005.
- de Viron, O., Boy, J.-P. & Goosse, H., 2004. Geodetic effects of the ocean response to atmospheric forcing in an ocean general circulation model, *J. geophys. Res.*, **109**, doi:10.1029/2003JB002837.
- Degnan, J., 1993. Millimeter accuracy satellite laser ranging: a review, contributions of space geodesy to geodynamics: technology, *Geodynamics*, **25**, 133–162.
- Dong, D., Herring, T.A. & King, R.W., 1998. Estimating regional deformation from a combination of space and terrestrial geodetic data, *J. Geodesy*, **72**, 200–214.
- Dong, D., Fang, P., Bock, Y., Cheng, M.K. & Miyasaki, S., 2002. Anatomy of apparent seasonal variations from GPS-derived site position time series, *J. geophys. Res.*, **107**, doi:10.1029/2001JB000573.
- Eanes, R.J. & Schuler, A., 1999. An improved global ocean tide model from TOPEX/Poseidon altimetry: CSR4.O, in *EGS, 24th General Assembly*, The Hague (NL), 1999.
- Ekman, M. & Mäkinen, J., 1996. Recent postglacial rebound, gravity change and mantle flow in Fennoscandia, *Geophys. J. Int.*, **126**, 229–234.
- Farrell, W.E., 1972. Deformation of the Earth by surface loads, *Reviews of Geophysics and Space Physics*, **10**, 761–797.
- Feigl, K.L. et al., 1993. Space geodetic measurement of crustal deformation in central and southern California, 1984–1992, *J. geophys. Res.*, **98**(B12), 21 677–21 712, doi:10.1029/93JB02405.
- Francis, O., Van Camp, M., van Dam, T., Warnant, R. & Hendrickx, M., 2004. Indication of the uplift of the Ardennes in long term gravity variations in Membach (Belgium), *Geophys. J. Int.*, **158**, 346–352.
- Gilli, E., 2002. Recherche de causes potentielles de variations gravimétriques dans l'endokarst du plateau de Calern, *AGRET - 1999–2001*, 93–103.
- Hinderer, J., Legros, H. & Crossley, D.J., 1991. Global Earth dynamics and induced gravity changes, *J. geophys. Res.*, **96**, 20 257–20 265.
- Hugentobler, U. et al., 1999. CODE IGS Analysis Center Technical Report 1999.
- Hugentobler, U. et al., 2000. CODE IGS Analysis Center Technical Report 2000.
- Hugentobler, U. et al., 2002. CODE IGS Analysis Center Technical Report 2002.
- King, R.W. & Bock, Y., 2005. Documentation for the GAMIT GPS software analysis, release 10.05, *Mass. Inst. of Technol. Cambridge*.
- Lambert, A., Courtier, N. & Brown, J.M., 2002. Estimating local seasonal variations in the water content of soil by measuring variations gravitational attraction, *Proceedings Canadian Geophysical Union*.
- Lefèvre, F., Lyard, F., Provost, C.L. & Schrama, E., 2002. FES99: A global tide finite element solution assimilating tide gauge and altimetric information, *J. Atm. Oceanic Tech.*, **19**, 1345–1356.
- Llubes, M., Florsch, N., Hinderer, J., Longuevergne, L. & Amalvict, M., 2004. Local hydrology, the Global geodynamics Project and CHAMP/GRACE perspective: some case studies, *J. Geodyn.*, **38**, 355–354.
- MacMillan, D.S. & Gipson, J.M., 1994. Atmospheric pressure loading parameters from very long baseline interferometry observations, *J. geophys. Res.*, **99**, 18 081–18 087.
- Mangiarotti, S., Cazenave, A., Soudarin, L. & Crétaux, J.F., 2001. Annual vertical crustal motions predicted from surface mass redistribution and observed by space geodesy, *J. geophys. Res.*, **106**, 4277–4291.
- McCarthy, D., 1996. IERS Conventions (1996), *IERS Technical Note*, Paris, July 1996.
- McCarthy, D.D. & Petit, G., 2004. IERS Conventions (2003), *IERS Technical Note*, 32 Frankfurt am Main: Verlag des Bundesamts für Kartographie und Geodäsie. 127 p., paperback, ISBN 3–89888–884–3.
- Micro-g Solutions Inc., 2004. 'g' 4.00 absolute gravity data acquisition and processing, Micro-g Solutions Inc., Lafayette, Colorado, USA, March 2004.
- Milly, P.C.D. & Shmakin, A.B., 2002. Global modeling of land water and energy balances. Part I: the land dynamics (LaD) model, *J. Hydrometeorology*, **3**, 283–299.
- Nicolas, J., Bonnefond, P., Laurain, O., Pierron, F., Exertier, P. & Barlier, F., 2002. Triple laser ranging collocation experiment at the Grasse observatory, France—September–November 2001, *13th International Workshop on Laser Ranging 'Towards Millimeter Accuracy'*, Washington USA, 7–11 October 2002.
- Niebauer, T.M., Sasagawa, G.S., Faller, J.E., Hilt, R. & Klopping, F., 1995. A new generation of absolute gravimeters, *Metrologia*, **32**, 159–180.
- Niell, A.E., 1996. Global mapping functions for the atmosphere delay at radio wavelengths, *J. geophys. Res.*, **101**, 3227–3246.
- Nocquet, J.-M. & Calais, E., 2003. Crustal velocity field of Western Europe from permanent GPS array solutions, 1996–2001, *Geophys. J. Int.*, **154**, 72–88.
- Nocquet, J.-M., Willis, P. & Garcia, S., 2006. Plate kinematics of Nubia–Somalia using a combined DORIS and GPS solutions, *J. Geodesy*, in press, doi:10.1007/s00190-006-0078-0.
- Rabbel, W. & Zschau, J., 1985. Static deformations and gravity changes at the earth's surface due to atmospheric loading, *J. Geophys.*, **56**, 81–99.
- Richter, B., Zerbini, S., Matonti, F. & Simon, D., 2004. Long-term crustal deformation monitored by gravity and space techniques at Medicina, Italy and Wettzell, Germany, *J. Geodyn.*, **38**, 281–292.
- Rodell, M. et al., 2004. The global land data assimilation system, *Bull. Amer. Meteor. Soc.*, doi:10.1175/BAMS-85-3-381, pp. 381–394.
- Rothacher, M. & Mader, G., 2003. Receiver and satellite antenna phase center offsets and variations, in *Proc. IGS 2002 Network, Data and Analysis Centre Workshop*, pp. 141–152, eds Tetreault, P., Neilan, R. & Gowey, K., Ottawa, Canada.
- Rothacher, M. et al., 1998. Annual Report 1998 of the CODE Analysis Center of the IGS, University of Bern.
- Scherneck, H.-G., 1991. A parametrized solid earth tide model and ocean tide loading effects for global geodetic baseline measurements, *Geophys. J. Int.*, **106**, 677–694.

- Sperl, M., 1998. Period98, *Commun. Asteroeismology* (M. Breger ed., Austrian Academy of Sciences, Vienna), 111.
- Tregoning, P. & van Dam, T., 2005. Effects of atmospheric pressure loading and seven-parameter transformations on estimates of geocenter motion and station heights from space geodetic observations, *J. geophys. Res.*, **110**, B03408, doi:10.1029/2004JB003334.
- Van Camp, M., Hendrickx, M., Richard, P., Thies, S., Hinderer, J., Amalvict, M., Luck, B. & Falk, R., 2003. Comparison of the FG5#101, #202, #206 and #209 absolute gravimeters at four different European sites, *Cahier du Centre Européen de Géodynamique et de Séismologie, Luxembourg*, **22**, 65–73.
- Van Camp, M., Williams, S.D.P. & Francis, O., 2005. Uncertainty of absolute gravity measurements, *J. geophys. Res.*, **110**, B05406, doi:10.1029/2004JB003497.
- van Dam, T.M. & Herring, T.A., 1994. Detection of atmospheric pressure loading using very long baseline interferometry measurements, *J. geophys. Res.*, **99**, 4505–4517.
- van Dam, T.M. & Wahr, J.M., 1987. Displacements of the Earth's surface due to atmospheric loading: effects on gravity and baseline measurements, *J. geophys. Res.*, **92**, 1281–1286.
- van Dam, T.M. & Wahr, J.M., 1998. Modeling environment loading effects: a review, *Phys. Chem. Earth*, **23**, 1077–1087.
- van Dam, T.M., Blewitt, G. & Heflin, M.B., 1994. Atmospheric pressure loading effects on Global Positioning System coordinate determinations, *J. geophys. Res.*, **99**, 23 939–23 950.
- van Dam, T.M., Wahr, J.M., Chao, Y. & Leuliette, E., 1997. Predictions of crustal deformation and of geoid and sea-level variability caused by oceanic and atmospheric loading, *Geophys. J. Int.*, **129**, 507–517.
- van Dam, T., Wahr, J., Milly, P.C.D., Shmakin, A.B., Blewitt, G., Lavallée, D. & Larson, K.M., 2001. Crustal displacements due to continental water loading, *Geophys. Res. Lett.*, **28**, 651–654.
- van Dam, T., Plag, H.-P., Francis, O. & Gegout, P., 2002. GGFC Special Bureau for loading: current Status and Plans.
- Wahr, J.M., 1985. Deformation induced by polar motion, *J. geophys. Res.*, **90**, 9363–9368.
- Williams, S.D.P., Bock, Y., Fang, P., Jamason, P., Nikolaidis, R.M., Prawirodirdjo, L., Miller, M. & Johnson, D.J., 2004. Error analysis of continuous GPS position time series, *J. geophys. Res.*, **109**, B03412, doi:10.1029/2003JB002741.
- Zerbini, S., Richter, B., Negusini, M., Romagnoli, C., Simon, D., Domenichini, F. & Schwahn, W., 2001. Height and gravity variations by continuous GPS, gravity and environmental parameter observations in the southern Po plain, near Bologna, Italy, *Earth planet. Sci. Lett.*, **192**, 267–279.